

Research on the Design of Power Supply Gateway and Wireless Power Transmission Based on Edge Computing

Zemin Wang, Zhejiang Energy Group R&D Institution Co., Ltd., China*

Jianmiao Ping, Zhejiang Energy Group R&D Institution Co., Ltd., China

Junwei Fu, Zhejiang Energy Group R&D Institution Co., Ltd., China

Yuedeng He, Zhejiang Energy Group R&D Institution Co., Ltd., China

Changchun Li, Zhejiang Energy Group R&D Institution Co., Ltd., China

ABSTRACT

There is a rising need for sensors under an IoT network to identify and monitor the environment as more IoT devices and services are made accessible for use. This movement presents challenges such as the proliferation of data and the scarcity of energy. This research presents a strategy for enhancing the service provision capabilities of WSN-aided IoT applications by combining mobile edge computation with wireless signal and control transmission. In order to reduce overall system energy consumption while maintaining data transmission rate and power needs, a new optimization problem integrating power allocation, CPU frequency, offloading weight factor, and energy harvesting is devised. The non-convex nature of the problem necessitates the development of a novel ideal solution group iterative process optimization model that divides the original problem into multiple subproblems, with each subproblem being optimized in turn. According to the results of simulations with a numerical model, our proposed method consumes considerably less energy than just the two benchmark methodologies.

KEYWORDS

Edge Computing, Energy Minimization, IoT, Power Transfer, Wireless Sensing Network

INTRODUCTION

With the 5G-enabled Internet of Things (IoT) (Shafique et al., 2020), humans can connect their physical environments with their digital environments at a time when human civilization is transitioning from informatization to intelligence (Chettri & Bera, 2019). Big capacity, ultralow latency, high dependability, and broad connectivity are the four qualities of the 5G communication system that are most significant for the development of IoT (Shahzadi et al., 2019). Using IoT services is now possible not just in smart cities (Wang et al., 2018) but also agriculture (Xuefei et al., 2020), medical care (Wazid et al., 2020), transportation (Dua et al., 2020), industry (Lu et al., 2020), and other fields

DOI: 10.4018/IJDST.340941

*Corresponding Author

This article published as an Open Access article distributed under the terms of the Creative Commons Attribution License (<http://creativecommons.org/licenses/by/4.0/>) which permits unrestricted use, distribution, and production in any medium, provided the author of the original work and original publication source are properly credited.

(Zhang et al., 2020). Because 5G and wireless sensor network (WSN)-assisted IoT make it a lot easier to link the physical world with the internet (Lu et al., 2020), this is the case. Although WSN-assisted IoT presents significant risks (Zhang et al., 2020), the vast amounts of data traffic generated by a massive number of IoT devices and sensor systems may place considerable strain on the network (Cui et al., 2021), resulting in increased service disruptions and significantly reduced quality of service (QoS) (Jiang et al., 2020).

Regardless of the fact that technologically advanced terminal systems are dealing with advanced technology (Hewa et al., 2020), meeting the expectations of a computing-intensive workforce, specifically when it comes to ensuring low resource utilization and latency, can be difficult. Throughout the 5G IoT, multi-access edge computing (MEC), aka mobile edge computing technology, has been widely recognized as a significant framework (Zhang et al., 2016). In addition to reducing their own processing impact and energy efficiency (Spinelli & Mancuso, 2020), terminal appliances can offload almost all of their computational operations to an edge cloud infrastructure for processing (Spinelli & Mancuso, 2020), thereby increasing the processing productivity and effectiveness of the computing device while also providing a higher level of service (Liu et al., 2020). When MEC enabled industrial areas of expertise to continue operating in 5G environments, Guo et al. (2017) examined how this was accomplished. Giannopoulos et al. (2021) cite a study by Yang et al. that looked into the essential characteristics of MEC throughout the context of 5G as well as IoT. They also identified and described numerous fundamental core technologies that would allow MEC to be included in 5G and IoT.

IoT continues to face a difficult obstacle, regardless of the fact that MEC offers huge benefits. The question is, how the life expectancy of IoT devices connected to the network be quickly and effectively extended? The simultaneous wireless information and power transmission (SWIPT) technology has been the most hopeful way to solve this issue. The SWIPT system is based on the concept that radio frequency (RF) transmitters can carry both energy and relevant data at the same time, which is supported by research. Balaji and Nivedha (2021) first suggested this concept in 2021. Two practical SWIPT receiver systems, such as the time switching (TS) receiver and the power splitting (PS) recipient, were presented by Rui Zhang and colleagues (Tang et al., 2017). The TS receiver divides the time slot into two different halves, mostly with RF received signals in the first half of the time frame being used to process information demodulation as well as the signal gathered. In the second half of the time frame, energy harvesting is being used. Specifically, to fulfill both information demodulation and energy generation at the same time, the PS receiver divides the received RF signal into different components and feeds every component toward the energy collector as well as the information demodulator separately (Fu et al., 2020), whereupon the experiment is repeated. Following this discovery, a considerable number of research studies have been conducted that have focused on the quality and implementation of SWIPT systems (Zhou et al., 2018).

This paper is based on the preceding two receivers, and it proposes a more complex dynamic energy partitioning receiver in accordance with the work of Ksentini and Frangoudis (2020). Regarding SWIPT sensing devices, Balaji and Krishnan (2021) looked at the trade-off involving energy use and data transmission. Min et al. (2019) refer to Ting et al., who developed TS receivers for the IoT to provide energy efficiency measures in multiple-input, multiple-output (MIMO) channels.

Developing MEC-deployed WSN IoT infrastructure in cooperation with SWIPT is becoming increasingly popular because both SWIPT and MEC technologies are useful to the IoT technology system. To improve performance of the system in this general paradigm, optimizing the deployment of storage and computational resources, or even the deployment of a wireless energy harvesting technique, is necessary. Lu et al. (2020) explored an energy efficiency optimization technique for orthogonal frequency division multiplexing (OFDM) transmission in the context of smart agricultural production using OFDM transmission WSN. The Growth-based systems may aid in the resolution of issues of energy shortage by optimizing both the received power and the pairing of subcarriers at almost the same time, which may reduce the amount of energy consumed. To address the limits in storage capacity

and computational power of IoT terminals, Zhang et al. (2020) proposed a realistic rate maximization problem for a multiple user satellite IoT system with SWIPT and MEC. In accordance with Chen et al. (2019), the remaining sections of Zhang et al.'s (2020) paper are organized as follows. Balaji and Krishnan (2021) investigated the feasibility of a remote-controlled system. The offloading modes of an unmanned aerial vehicle (UAV)-enabled remotely driven MEC system were investigated, and the offloading mechanisms were optimized to obtain the best achievable compute rate while maintaining the power and recommended UAV speed limitations. Zhou et al. (2020) were able to improve MEC by incorporating the long range (LoRa) technology for IoT applications with the assistance of work done by Mao et al. (2016). Because of its modular design, the conceptual framework enables dynamic IoT implementation at the edge, along with life cycle management for connected devices.

The advancement of artificial intelligence technology has resulted in the adoption of reinforcement learning (RL) methodologies to handle a variety of communication challenges in 5G and IoT systems. Balaji et al. (2021) described a unique deep reinforcement learning (DRL) strategy with the goal of decreasing the discrepancy between the dispersed and desired throughput for each user while also satisfying the user needs via power regulation. Balaji et al. (2021) investigated an RL-based offloading system for IoT devices, with the goal of determining the best edge device and offloading rate. The RL-based offloading system's unique characteristic is that it allows for the optimization of the offloading technique without the requirement for prior knowledge; much more conventional systems did not have this capacity. The system presented a hybrid decision-based DRL strategy for offering integrated choices of dynamically offloading strategies for multi-device multi-server MEC-IoT systems that is based on combination decision-based DRL and thermoelectric materials.

This work examines energy consumption reduction for SWIPT-based MEC in a WSN-aided IoT system accomplished via the use of an optimization technique. It is a continuation of our prior study, which was primarily concerned with the cellular structure. Despite the fact that this research is centered on the WSN-aided IoT network, the findings are applicable to certain other IoT networks as well. A thorough examination was conducted compared with the earlier study to determine the effects of system power consumption on the amount of the computational workload, the number of mobile nodes (includes wireless sensor nodes), the quantity of antennas, and the energy harvest weighting factor. The following are some of the surprises included in this work. A unique WSN-assisted IoT system incorporates an anchor node (AN) that deploys both an MEC and full duplex (FD) system. Several SWIPT-equipped mobile nodes (MNs) were also developed. Because of transmission characteristics and requirements among a cellular communication network and a wireless technology are so diverse, the issue of the stage of the system is totally different from our previous research. We intend to reduce energy use as much as feasible by, among many other things, improving the CPU frequency, power allocation, offloading weight factor, and SWIPT weight factor. In addition, we offer a closed form equation for the downlink rate and even a closed form calculation for the downlink transmission delay, both of which are based on the analysis of the uplink study. Also being tweaked is the SWIPT weight matrix, which will have an effect on the energy use of data transmission harvesting and consequently the overall energy consumption of a mechanism. In this study, we offer a much more reliable framework of generating power that is completely reliant on the downlink time delay, which is based on the SWIPT weight factor and the downlink time delay, respectively. In other words, the uplink and downlink parameters are tuned in cooperation with one another to maximize throughput. The development of a more practicable WSN energy minimization issue by optimizing the system's primary decision variables in concert with one another has been accomplished through collaboration. This development is necessary because the different variables that need to be improved are interconnected, and the original problem is nonconvex, making optimization extremely challenging. In this paper, we describe the alternative group iteration optimization (AGIO) algorithm, which is a rapid and efficient method of optimization. Using this approach, we divide the original factors into smaller subproblems and divide the choice variables into three categories, each of which contains

three decision characteristics. We then use the interior point iteration strategy to alternately optimize each subproblem until the solution is found.

SYSTEM MODEL

Figure 1 depicts an example of a SWIPT-MEC supported WSN facilitated IoT system that is enabled by the MEC protocol. The current configuration includes N mobile nodes that incorporate wireless sensor nodes denoted by the letters $DN, D1, D2$, etc., which are constantly bombarded with computation tasks, and also one anchor node, which is furnished with M -antenna FD communications networks. Solar energy is collected by each MN using a single antenna and electricity partitioning SWIPT equipment, which is provided by the company. The PS receiver is capable of turning between the piezoelectric materials and the relevant data decoding states in timely manner, depending on the situation. The anchor system is connected with an MEC server that might be of assistance to MNs in dealing with the significant number of computational jobs that they are required to perform. In the event that each MN is able to divide its computational work into two components—one for local computing and the other for offloading to the MEC-equipped AN—the following generalizations can be made: When representing the entire computational and storage job size of D_i , we use line interface unit (LIU) bits, and when representing the offloading computation task size of D_i , we also use LIU bits. This corresponds to the equation $Liu = \alpha_i L_i$, where $0 < \alpha_i < 1$ is an offloading weight matrix. The fact that MN has the capabilities to choose what kind of computational effort will be delegated to the AN means that I is a parameter that should be resolved to increase efficiency. We describe the operating procedures of the system in this section and demonstrate them in the following phases:

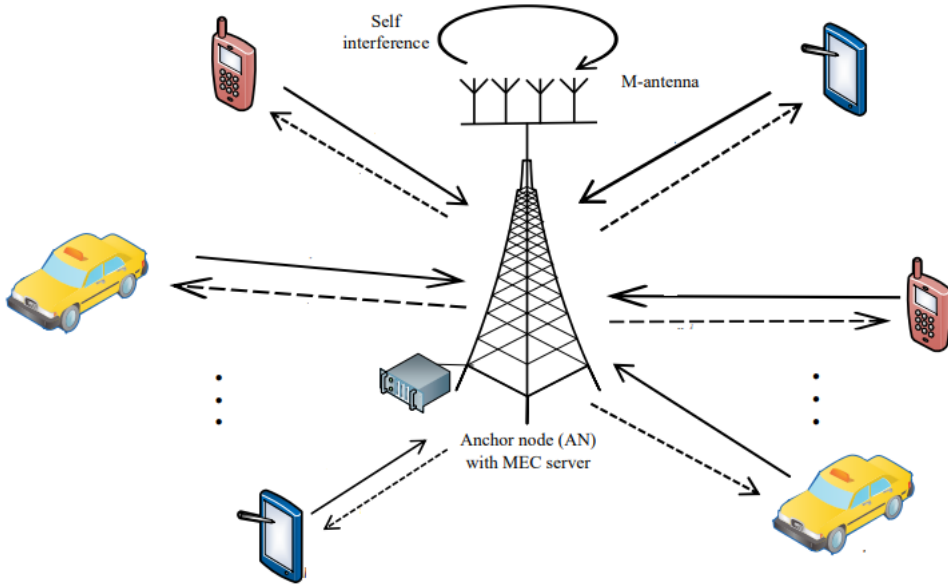
- During the uplink process, MN D_i ($i \in \{1, \dots, N\}$) offloads the calculation job Liu to the MEC server at AN.
- As soon as the MEC server gets the offloading job, it begins working on the computing task. Given its powerful calculation capabilities, the MEC server can complete offloading computation tasks in a short period of time that can be disregarded when compared with the rest of its operational time.
- Because AN uses FD technology when MN D_i is offloaded, the calculation result L_{jd} may be downloaded concurrently from the MEC server to MN D_j ($j \in \{1, \dots, N\}, j \neq i$), which operates on the same frequency as the uplink MN D_i . The output of the calculation meets the equation $L_{jd} = \beta_j Liu$, where $0 < \beta_j < 1$ is a weight factor.
- Following receipt of the computing result by D_j , the PS receiver will execute energy harvesting and information decoding in accordance with the received RF signal.
- When D_i has completed the offloading of the remaining computation work, it will undertake local computing on the remaining computation task.

The procedures described above can be separated into three phases: the offloading phase, the downloading phase, and the local computation phase. Each of them is discussed in further depth in the next section.

PHASE ONE: OFFLOADING PHASE

When MNs $\{D1, D2, \dots, DN\}$ become overburdened by the computing jobs, they will dump a portion of the tasks to AN, which will then process the remainder. Without sacrificing generality, AN gets the offloading computing job Liu from MN D_i throughout the time period t_{iu} , which is defined as the duration starting from the initiation of the offload request by MN D_i to the completion of the computation task by AN and the return of the results to MN D_i . At the same time, the AN concurrently uploads the calculation result L_{jd} to D_j , where $i \in \{1, \dots, N\}$ and $j \in \{1, \dots, N\}, i \neq j$ and the outcome

Figure 1. WSN-Aided IoT system model



of the computation is $6 = I \cdot 6$. In this case, the signal that was received at AN is calculated as shown in equation (1):

$$Y_j^u = \sqrt{P_i^u} H_i^u S_i^u + \sqrt{H_0} \left(\sqrt{P_j^d} S_j^d \right) + n_{AN} \quad (1)$$

Equation (1) is a mathematical expression that describes a communication system. The equation has three parts on the right-hand side. The first part represents the target offloading job, or the data that is being transmitted. The second part represents RF signal interference owing to FM transmission of AN, which can interfere with the transmission of the target offloading job. The third part represents additive white Gaussian noise generated at AN. This noise is caused by random variations in the wireless channel and can also interfere with the transmission of the target offloading job.

The transmitted power and transmitted signal of Di are denoted by P_j^d and S_j^d , respectively. The transmitted power and calculation result signals of AN are denoted by P_j^d , and the calculation result signal of AN is denoted by the transmitted power and calculation result signal of AN are denoted by P_j^d and calculation result signal of AN are denoted by the transmitted power and calculation result signal of AN are denoted by the transmitted power and calculation. Both transmitted signals are regarded to have normalized power in this situation, which is equal to 1 for $|S_i^u|^2 = 1$ for $|S_j^d|^2 = 1$ in this example. Although $H_i^u \in \mathbb{C}^{M \times 1}$ represents the uplink channel from Di to AN, $H_0 \in \mathbb{C}^{M \times M}$ represents the self-interference channel created by the FD broadcast. The coefficient of residual self-interference is indicated by the letter j in the equation. When this kind of noise is heard, it is referred to as $n_{AN} \sim \text{CN}(0, \sigma_{AN}^2 I_M)$ noise.

According to the previous formulation, only the first portion on the right side of equation (1) corresponds to the target offloading job S_i^u , whereas the second portion corresponds to the RSI owing to FM transmission of AN, and the third portion corresponds to the additive white Gaussian

noise generated at AN. An example of how the signal-to-interference-plus-noise ratio (SINR) might be stated numerically for this communication system is shown in equation (2):

$$\gamma_i^u = \frac{p_i^u \left\{ H_i^u \left(H_i^u \right)^H \right\}}{p_j^d \text{tr} \left\{ H_0 H_0^H \right\} + \sigma_{AN}^2} \quad (2)$$

The SINR is a measure of the quality of the received signal relative to the interference and noise in the channel. In equation (2), the numerator represents the power of the received signal, and the denominator represents the sum of the power of the interference and the noise. In addition, tr. denotes that the matrix trace is used.

Now we can calculate the transmission rate using the formula shown in equation (3):

$$R_i^u = B \log_2 \left(1 + \gamma_i^u \right) \quad (3)$$

Equation (3) can be used to determine the transmission rate of the system. In this equation, B denotes the bandwidth of the channel,.

B specifies the amount of bandwidth that has been allocated, so we assume that R_{\min}^u is the required minimum uplink transmission rate for the application. As a result, we may arrive at the first restriction condition in this case. Equation (4) shows the calculation used for the system model:

$$R_i^u \geq R_{\min}^u \quad (4)$$

Equation (4) represents the required minimum uplink transmission rate for the application . This rate specifies the minimum amount of data that needs to be transmitted from the user device to the network in a given time period. It is a crucial parameter for ensuring the efficient functioning of the application.

Meanwhile, we use the formula shown in equation (5) to compute the transmission time required for offloading:

$$t_i^u = \frac{L_i^u}{R_i^u} \quad (5)$$

The transmission time is the duration it takes to transmit a certain amount of data from the user device to the network. This calculation is essential for understanding the timing and efficiency of the offloading process within the system model.

This means that Di's total energy consumption throughout the offloading phase may be represented as shown in equations (6) and (7):

$$E_i^{off} = p_i^u \frac{L_i^u}{R_i^u} \quad (6)$$

$$E_i^{off} = \sum_{i=1}^N E_i^{off} \quad (7)$$

PHASE TWO: DOWNLOADING PHASE

Given that AN is equipped with FD technology, it can concurrently download the computation output to MN Dj while also receiving offloading tasks from other MN Di. As a result, the signal is received at Dj. The formula shown in equation (8) explains what it is.

$$y_j^d = \sqrt{P_j^d} H_j^d S_j^d + n_j^d \quad (8)$$

Equation (8) represents the signal received at device (D_j), which is denoted as (y_j) in the context of AN's FD technology. FD technology allows AN to transmit and receive signals simultaneously on the same frequency band.

In this case p_j^d is the amount of transferred power that AN uses to transfer the compute result to Dj. n_j^d is the AWGN with a lot of power σ_j^2 . In this case, we assume that the co-channel interference can be completely canceled in the receiver. Finally, the SINR and the transmission rate at a given distance are calculated, as shown in equations (9) and (10). The following are the MN Dj:

$$\gamma_j^d = \frac{p_j^d \text{tr} \left\{ H_j^d \left(H_j^d \right)^H \right\}}{\sigma_j^2} \quad (9)$$

$$R_j^d = B \log_2 \left(1 + \gamma_j^d \right) \quad (10)$$

Equation (9) represents the SINR at device (D_j) when AN transfers the computed result to (D_j). The term (β) denotes the amount of power transferred by AN for this purpose, and (N) represents the additive white Gaussian noise (AWGN) power in the channel. In this case, we assume that co-channel interference can be completely canceled at the receiver, enhancing the quality of the received signal.

Equation (10) calculates the transmission rate at a given distance for the communication link between AN and device (D_j). The formula uses the SINR calculated in equation (9) to determine the achievable transmission rate based on the channel conditions and the amount of power allocated for transmission.

For the sake of simplicity, let R_{\min}^d shown in equation (11) represent the minimal downlink transmission rate required to achieve another constraint condition that is explained in the next paragraph:

$$R_j^d \geq R_{\min}^d \quad (11)$$

The constraint condition in equation (11) helps ensure that the communication link between AN and device (D_j) can support the necessary data transfer rate for the intended applications.

Now we compute the delay of the downlink transmission using the formula shown in equation (12):

$$t_j^d = \frac{L_j^d}{R_j^d} \quad (12)$$

Equation (12) provides insights into the time it takes for data to be successfully transmitted from AN to device (D_j) over the wireless link.

Once the RF signal has been received by D_j, the PS receiver separates it into two parts. The first component ($0 \leq \theta \leq 1$) is used for energy harvesting, and the second part ($1 - \theta_j$) is used for data transmission. As a process of deciphering information, the harvest energy of D_j may be obtained using the formulas shown in equations (13) and (14):

$$E_j^{hav} = \theta_j \left(p_j^d \text{tr} \left\{ H_j^d \left(H_j^d \right)^H \right\} + \sigma_j^2 \right) t_j^d \quad (13)$$

$$E_{AN} = \sum_{j=1}^N p_i^d t_i^d \quad (14)$$

Equations (13) and (14) describe the energy harvesting process at device (D_j) once the RF signal is received. Equation (13) computes the harvested energy ((E_h)) based on the amount of power allocated for energy harvesting ((η)) and the received signal power ((P_r)). Equation (14) calculates the energy used for data transmission ((E_d)) based on the remaining power after energy harvesting (($1 - \eta$)) and the transmission rate ((R)).

PHASE THREE: LOCAL COMPUTATION

Following the offloading of the computing job, MN continues to work on the remaining computation task. Let's say f_i^n is the case. Distinguishing between the D_i's nth CPU cycle necessitates a high frequency of the CPU. This constraint condition is set using the formula shown in equation (15):

$$0 \leq f_i^n \leq f_i^{\max}, I \quad (15)$$

In phase III, MN continues to perform the remaining computation task locally after offloading part of the computation job to AN. In this phase, equation (15) sets a constraint condition that ensures that each CPU cycle of device (D_i) requires a minimum frequency ((f_{\min})) and a maximum frequency ((f_{\max})), where (I) represents the number of CPU cycles required for the local computation.

In equation (15), f_i^{\max} is the maximum CPU frequency that D_i may operate at. Therefore, the the time required for the local calculation of D_i is shown in equations (16) and (17):

$$t_i^{loc} = \sum_{n=1}^{C(L_i - L_i^e)} \frac{1}{f_i^n} \quad (16)$$

$$E_i^{loc} = \sum_{n=1}^{C(L_i - L_i^e)} k \left(f_i^n \right)^2 \quad (17)$$

Equation (16) calculates the time required for local computation at device (D_i) based on the number of CPU cycles ((I)) and the clock frequency ((f_i)). Equation (17) uses the time calculated in equation (16) to determine the overall energy consumed by device (D_i) for local computation, taking into account the effective capacitance coefficient ((C_i)) of the chip architecture.

The effective capacitance coefficient depending on the chip architecture is denoted by the symbol. As a result, we can calculate the overall local energy consumption using the formula shown in equation (18).

$$E_i^{loc} = \sum_{i=1}^N E_i^{loc} \quad (18)$$

Equation (18) provides a formula for calculating the overall energy consumption of device (D_i) for both offloaded computation and local computation, allowing for the evaluation of the energy efficiency of the proposed computation offloading scheme.

PROJECTED SYSTEM

In the following sections we break down the problem into stages, each of which are addressed one at a time. The initial issue (P1) presents a number of difficult problems owing to the fact that both the optimization problem and the limitations are non-convex. Even though all of the variables that need to be optimized are linked together in P1, we investigate that the CPU frequency f is by far the least significant of all the variables. To illustrate local computation optimization, consider the following scenario: When solving this subproblem, we employ the technique described in Liu et al. (2022) to determine the optimal CPU frequency.

The term “power optimization” refers to the following definition: When f and the weight factors are both fixed, we can use the interior point approach to solve the problem at hand. To achieve weight factor optimization, several approaches can be used. It is possible to use the interior point approach to produce the optimal weight factors after the frequency and power optimization has been completed.

It is possible to optimize weight factors by using an iterative method to find the optimal solution, using a branch and bound algorithm to solve the problem, or using convex optimization techniques to approximate the solution.

Weight factor optimization is managed in the following manner: First, we use the interior point approach to solve for the optimal frequency and power values. Then, we use one of the aforementioned methods to optimize the weight factors. Finally, we repeat this process until a satisfactory solution is obtained.

We recommend that the recursive approach could have been used to enhance the three subgoals in a sequential fashion. By breaking down the problem into these subproblems and addressing them in a systematic way, we can effectively optimize P1 despite its non-convexity.

Optimization of Local Computation

According to Liu et al. (2022), the best CPU frequency should fulfil the requirements shown in equation (19):

$$f_i^1 = f_i^2 = \dots = f_i^{C(L_i - E_i^a)} = \bar{f}_i \quad (19)$$

Equation (19) specifies that the CPU frequency (f_i) should remain constant throughout each cycle (I). This constraint ensures that the CPU operates at a consistent frequency level for the duration of the computation task, enhancing computational efficiency.

In accordance with equation (19), the CPU frequency should remain constant during each cycle as \bar{f}_i . The following is an example of how the original issue (P1) may be rewritten if the other four variables have been optimized.

Problem 1:

Min E^{tot} with C1 to C7

Problem 2:

$$\text{Min } E + \sum_{i=1}^N C(L_i - L_i^u) k(\bar{f}_i)^2$$

$$E = E^{\text{AN}} + E^{\text{off}} - E^{\text{hav}}$$

$$\bar{f} = [\bar{f}_1, \bar{f}_2, \dots, \bar{f}_N]$$

According to the objective function of optimization, the energy consumption rises in a monotonic manner as f_i grows. In other words, f_i must be the smallest possible number to obtain the lowest possible energy use. As a result of the constraint C6, we can get the results shown in equations (20) and (21):

$$f_i^{\text{opt}} = \frac{C(L_i - L_i^u)}{t_i^u} \quad (20)$$

$$E_i^{\text{loc}} = \frac{kC^3(L_i - L_i^u)^3}{(t_i^u)^2} \quad (21)$$

Equation (20) calculates the optimal CPU frequency (f_i) as the average of the minimum and maximum frequencies allowed, ensuring that the CPU operates within the specified frequency range. Equation (21) determines the number of CPU cycles required ((I)) based on the computation time ((T_{comp})) and the inverse of the CPU frequency, rounded up to the nearest integer to account for the discrete nature of CPU cycles. These equations help in optimizing the local computation process to achieve efficient energy utilization and computational performance.

Optimization of Power

If we assume that the CPU frequency has been improved and that the two weight factors have also been optimized, the solution to problem P1 may be recast in the following way:

Problem 3:

$$\text{Min } \sum_{j=1}^N p_j^d \frac{L_j^d}{R_j^d} + \sum_{i=1}^N p_i^u \frac{L_i^u}{R_i^u} + \sum_{i=1}^N \frac{kC^3(L_i - L_i^u)^3}{(t_i^u)^2} - \sum_{j=1}^N (p_j^d \text{tr} \{H_j^d (H_j^d)^H\} + \sigma_j^2) \frac{L_j^d}{R_j^d} \quad (22)$$

In the case of problem 3, the second-order derivative of each variable of the objective function is equal to 1, as shown in equation (22). Furthermore, all restrictions are linear in nature. Thus, we can apply the conventional interior point method to this convex issue and obtain the optimum solution.

Optimization of Weight Factor

Equation (23) shows an expression for the issue using the optimized variables f , p_u , and p_d :

Problem 4:

$$\text{Min} \sum_{j=1}^N p_j^d \frac{\beta_j \alpha_i L_i}{R_j^d} + \sum_{i=1}^N p_i^d \frac{\alpha_i L_i}{R_i^u} + \sum_{i=1}^N \frac{kC^3 (L_i - L_i^u)^3}{(L_i^u)^2} - \sum_{j=1}^N (p_j^d + \sigma_j^2) \frac{\beta_j \alpha_i L_i}{R_j^d} \quad (23)$$

SIMULATION RESULTS

We simulated the work of previous studies and explored the impacts of various factors on the system performance. The following are the simulation parameters in their simplest form: There was a bandwidth of 5 MHz; the highest limits of transmission power were 5.2 W and 20.5 W; the weight factors were 1.3; and the noise power was -120.4 dBm. The chip effective capacitance coefficient was set to a value of 10.1–20, and the CPU cycles were set to a value of $C = 10.23$ cycles/bit. We used a random Rayleigh fading channel model for all the channel matrices in the simulation, and this model was used throughout. Furthermore, we compared the new AGIO method with two benchmark algorithms that were previously developed: the fixed-variable (FV) method and the full-offloading (FO) method.

With six MNs and an antenna number of six, Figure 2 illustrates the convergence performance of the proposed AGIO algorithm for various compute job sizes L (4, 8, and 12 M bits) with six MNs and an antenna number of six (AN). Following five rounds under variable L , the algorithm converged, as shown in Figure 2. This graph shows that our algorithm is successful. In addition, the convergence curves show that the energy consumption grows with the size of the calculation work L .

Figure 3 shows the results of our analysis of energy consumption of the system using three different algorithms and a variety of AN antennas M . In all the cases tested, the suggested AGIO algorithm consumed the least amount of system energy,

The energy consumption of the FO method and the suggested AGIO algorithm was significantly decreased when M was used. As a consequence, our algorithm predicted that the number of AN antennas would rise, resulting in a higher improvement in performance and lower energy use. As a result, we infer that the suggested AGIO algorithm is appropriate for AN with multiple antennas.

Figure 4 compares and contrasts the three distinct approaches when varied numbers of MNs were used. When the number of customers rose, the energy consumption increased as well, which may be related to the increasing amount of compute jobs that must be performed. Once again, the suggested AGIO algorithm surpassed both the FV and FO methods in terms of performance. The superiority of the proposed method rose in relation to the number of mins at a time, showing its suitability for use in multi-user situations.

Figure 5 shows the energy use of the three algorithms when the harvest weight factor is varied with N values of 2 and 4, respectively. The energy use of the three methods decreased when the parameter was increased or decreased. The FO and AGIO algorithms experienced a more pronounced decrease in significance compared to the FV algorithm due to their enhanced energy harvesting capacity. A higher value of α indicates greater harvested energy and lower overall system energy consumption than the FV algorithm. Consequently, we can infer that MN prefers to offload a larger portion of processing bits to AN in order to optimize energy efficiency.

Figure 6 shows the unloading delay of mins at a time in the uplink. The FV scheme outperformed the FO method by a little margin because we set the offloading weight factor = 0.025 for FV, which

Figure 2. Suggested AGIO algorithm's convergence behavior

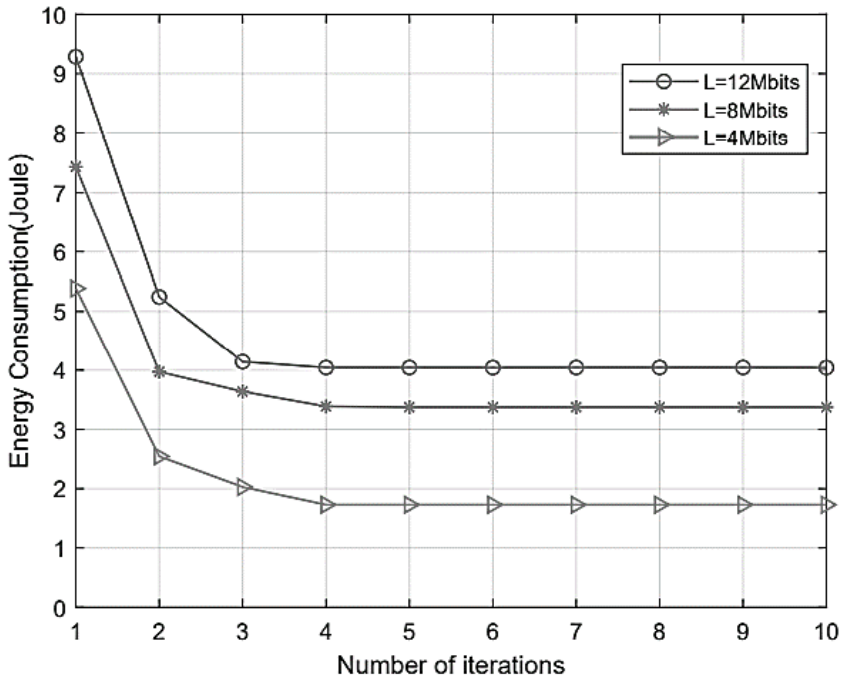
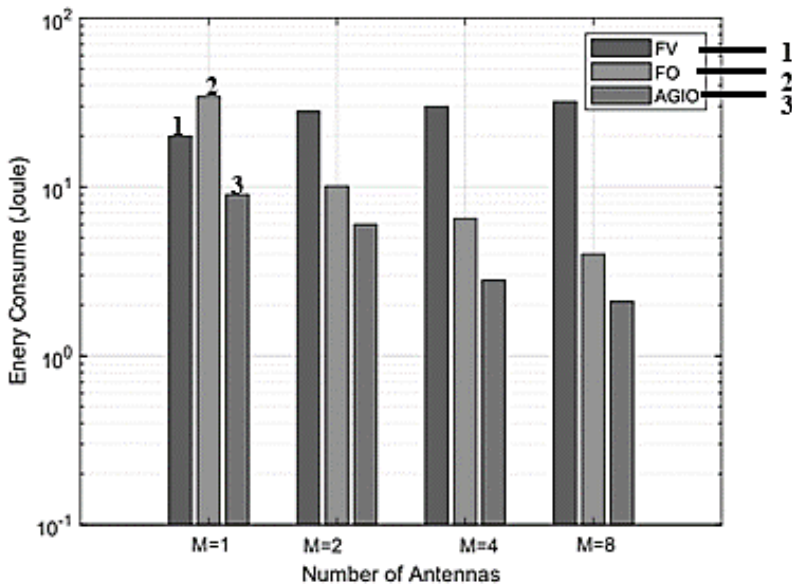


Figure 3. Energy consumption comparison



indicates that the offloading work in FV is less than the offloading task in FO. The AGIO method outperformed the two benchmarking algorithms in terms of latency performance, which may be attributed to the outstanding design of the optimization phases in the algorithm. It also demonstrates

Figure 4. Energy consumption comparison

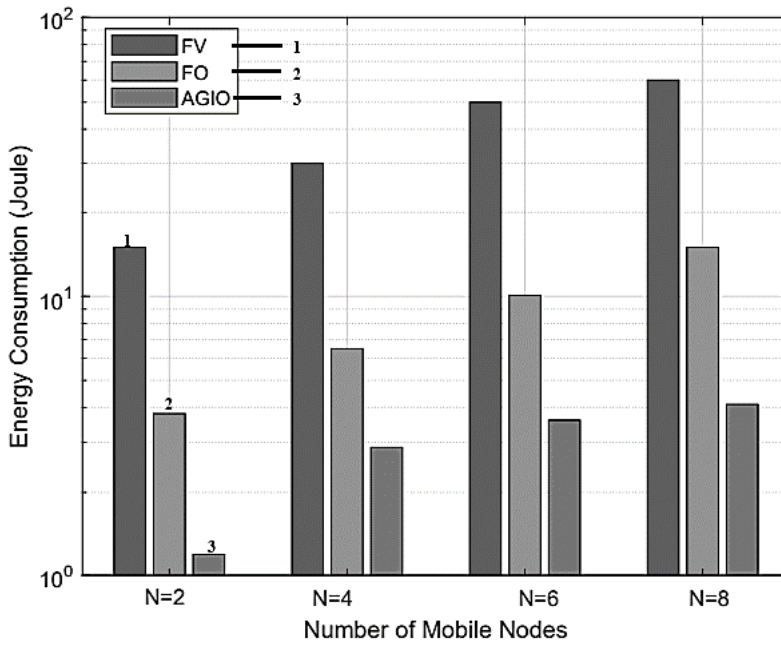
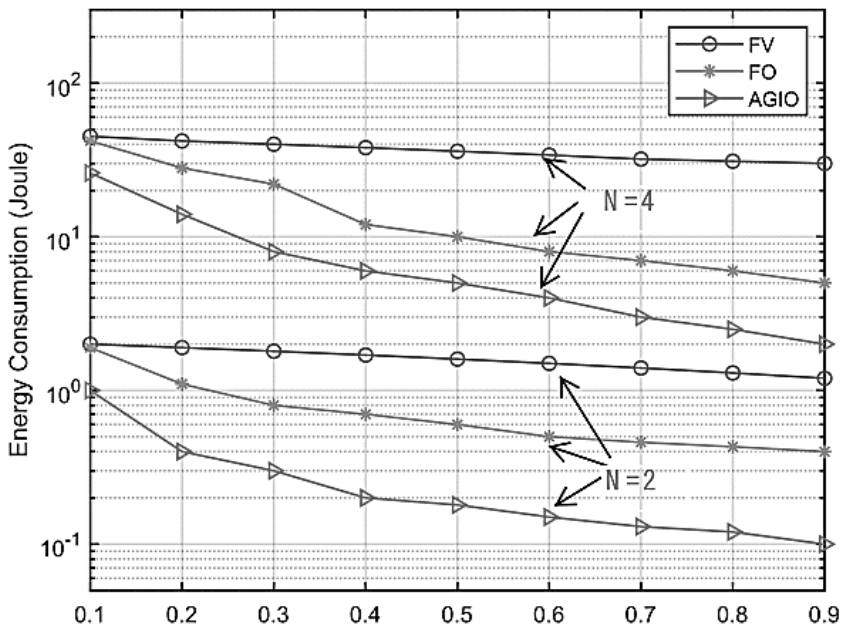


Figure 5. With different θ , energy consumption comparison



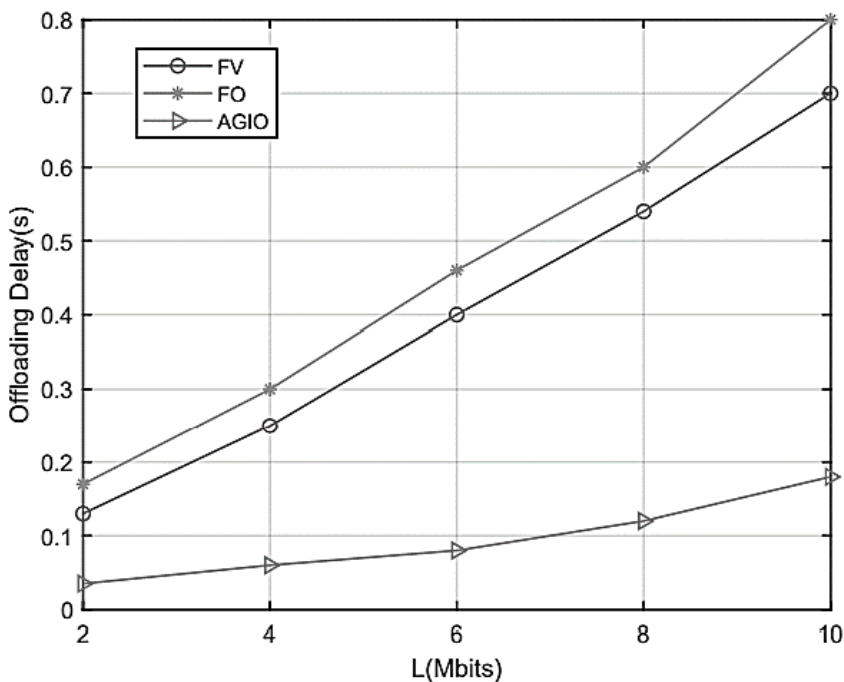
a distinguishing element of our algorithm's performance in terms of both energy consumption efficiency and latency efficiency.

Using MEC and SWIPT technology, we developed a novel framework for integrating an IoT system, with the purpose of overcoming the data explosion and energy insufficiency difficulties that users of WSN-assisted IoT systems have faced in the past. Our aim was to discuss the problem of energy consumption reduction and then provide an AGIO method for resolving the problem. By adjusting the CPU speed, power allocation, offloading mechanism, and SWIPT scheme in collaboration with one another, we achieved the minimal energy consumption level. In the end, the results of the simulation confirmed our initial intention. In the first place, as shown in Figures 5 and 6, the suggested revolutionary method offers substantial energy savings and time delay reductions over conventional systems. Several elements that have an impact on the overall performance of the system may have been more rationally formulated, and this may have contributed to its success. Additionally, the original donation contributes to the achievement of this aim. The resolution result presented in Figure 2 further verifies the use of the AGIO approach, which was previously explained in the second part of this paper. Additionally, the simulation results are shown in Figure 3, and they revealed that the energy consumption decreased as the number of AN antennas grew. The fact that our technology is suitable for multi-antenna systems, which are more efficient in terms of application efficiency, provides us a hint that our technology is on the right track. As shown in Figure 4, the simulation results indicate success of the suggested method in a multi-user environment, which corresponds to the real-world implementation of a wearable sensing IoT system in this work.

CONCLUSION

We investigated the wireless data transfer and energy transfer of a novel SWIPT-MEC enabled WSN-assisted IoT framework in this paper. During our simulation of an objective functions, we altered the CPU frequency, network throughput, offloading weight factor, and harvest weight factor all at the

Figure 6. Offloading delay comparison, different computation task size L



same time to achieve the lowest feasible system power consumption. We proposed a novel AGIO technique to achieve this goal. AGIO effectively breaks down the original problem into multiple subproblems, each of which can be optimized using group innermost express and communicate optimization techniques in a back-and-forth manner. Furthermore, we conducted a computational domain analysis of the proposed technique to assess it with the other two benchmark procedures in the literature. In this study, we demonstrated that the proposed architecture provides competitive advantages in terms of both energy consumption and latency.

DATA AVAILABILITY

The figures and tables used to support the findings of this study are included in the article.

CONFLICTS OF INTEREST

The authors declare that they have no conflicts of interest.

FUNDING STATEMENT

This work was not supported by any funds.

ACKNOWLEDGMENT

The authors would like to show sincere thanks to those techniques who have contributed to this research.

REFERENCES

- Balaji, B., & Ganesan, S. (2022). Power management in DC microgrid. In *Proceedings of International Conference on Power Electronics and Renewable Energy Systems: ICPERES 2021*, (pp. 213–225). Springer Singapore.
- Balaji, B., & Krishnan, D. S. (2021, May). FOPID controlled high step-up super lift DC-DC converter with enhanced response. In *Proceedings of the 2021 3rd International Conference on Signal Processing and Communication (ICSPSC)*, (pp. 176–179). IEEE. doi:10.1109/ICSPSC51351.2021.9451790
- Balaji, B., & Nivedha, S. (2021). Remote controlled road cleaning vehicle. *Journal of Physics: Conference Series*, 1717(1), 012014. doi:10.1088/1742-6596/1717/1/012014
- Balaji, B., Vengadesamani, B., & Sarvajith, M. (2021, May). Hysteresis controlled single-switch high step-up coupled-inductor boost converter. In *Proceedings of the 2021 3rd International Conference on Signal Processing and Communication (ICSPSC)*, (pp. 189–192). IEEE. doi:10.1109/ICSPSC51351.2021.9451745
- Chen, F., Fu, J., Wang, Z., Zhou, Y., & Qiu, W. (2019). Joint communication and computation resource optimization in FD-MEC cellular networks. *IEEE Access : Practical Innovations, Open Solutions*, 7, 168444–168454. doi:10.1109/ACCESS.2019.2954622
- Chettri, L., & Bera, R. (2020). A comprehensive survey on Internet of Things (IoT) toward 5G wireless systems. *IEEE Internet of Things Journal*, 7(1), 16–32. doi:10.1109/JIOT.2019.2948888
- Cui, J., Zhang, Y., Cao, M., Wang, S., & Xu, Y. (2021). RETRACTED: Thyroid tumour care risk based on medical IoT system. *Microprocessors and Microsystems*, 82(10), 103845. doi:10.1016/j.micpro.2021.103845
- Dua, A., Dutta, A., Zaman, N., & Kumar, N. (2020, July). Blockchain-based e-waste management in 5G smart communities. In *Proceedings of IEEE INFOCOM 2020 — IEEE Conference on Computer Communications Workshops (INFOCOM WKSHPS)*, (pp. 195–200). IEEE. doi:10.1109/INFOCOMWKSHPS50562.2020.9162845
- Editor-in-Chief of Microprocessor and Microsystems. (2023). Retraction notice to the articles published in the Special issue Signal Processing from “Microprocessors and Microsystems.”. *Microprocessors and Microsystems*, 101, 104901. doi:10.1016/j.micpro.2023.104901
- Fu, J., Hua, J., Wen, J., Zhou, K., Li, J., & Sheng, B. (2020). Optimization of achievable rate in the multiuser satellite IoT system with SWIPT and MEC. *IEEE Transactions on Industrial Informatics*, 17(3), 2072–2080. doi:10.1109/TII.2020.2985157
- Giannopoulos, A., Spantideas, S., Tsinos, C., & Trakadas, P. (2021, June). Power control in 5G heterogeneous cells considering user demands using deep reinforcement learning. In I. Maglogiannis, J. Macintyre, & L. Iliadis (Eds.), *Artificial intelligence applications and innovations. AIAI 2021 IFIP WG 12.5 international workshops. AIAI 2021. IFIP advances in information and communication technology*, 628 (pp. 95–105). Springer. doi:10.1007/978-3-030-79157-5_9
- Guo, S., Shi, Y., Yang, Y., & Xiao, B. (2017). Energy efficiency maximization in mobile wireless energy harvesting sensor networks. *IEEE Transactions on Mobile Computing*, 17(7), 1524–1537. doi:10.1109/TMC.2017.2773067
- Hewa, T., Braeken, A., Ylianttila, M., & Liyanage, M. (2020, December). Multi-access edge computing and blockchain-based secure telehealth system connected with 5G and IoT. In *Proceedings of GLOBECOM 2020 — 2020 IEEE Global Communications Conference*, (pp. 1–6). IEEE. doi:10.1109/GLOBECOM42002.2020.9348125
- Jiang, D., Wang, Z., Lv, Z., & Li, W. (2020, July). Smart antenna-based multi-hop highly-energy-efficient DSA approach to drone-assisted backhaul networks for 5G. In *Proceedings of IEEE INFOCOM 2020 — IEEE Conference on Computer Communications Workshops (INFOCOM WKSHPS)*, (pp. 883–887). IEEE. doi:10.1109/INFOCOMWKSHPS50562.2020.9162848
- Ksentini, A., & Frangoudis, P. A. (2020). On extending ETSI MEC to support LoRa for efficient IoT application deployment at the edge. *IEEE Communications Standards Magazine*, 4(2), 57–63. doi:10.1109/MCOMSTD.001.1900051

- Liu, C.-F., Bennis, M., Debbah, M., & Poor, H. V. (2019). Dynamic task offloading and resource allocation for ultra-reliable low-latency edge computing. *IEEE Transactions on Communications*, 67(6), 4132–4150. doi:10.1109/TCOMM.2019.2898573
- Liu, D., Liang, H., Zeng, X., Zhang, Q., Zhang, Z., & Li, M. (2022). Edge computing application, architecture, and challenges in ubiquitous power Internet of Things. *Frontiers in Energy Research*, 10, 850252. doi:10.3389/fenrg.2022.850252
- Liu, Y., Peng, M., Shou, G., Chen, Y., & Chen, S. (2020). Toward edge intelligence: Multiaccess edge computing for 5G and Internet of Things. *IEEE Internet of Things Journal*, 7(8), 6722–6747. doi:10.1109/JIOT.2020.3004500
- Lu, W., Xu, X., Huang, G., Li, B., Wu, Y., Zhao, N., & Yu, F. R. (2021). Energy efficiency optimization in SWIPT enabled WSNs for smart agriculture. *IEEE Transactions on Industrial Informatics*, 17(6), 4335–4344. doi:10.1109/TII.2020.2996672
- Lu, W., Xu, X., Ye, Q., Li, B., Peng, H., Hu, S., & Gong, Y. (2020). Power optimisation in UAV-assisted wireless powered cooperative mobile edge computing systems. *IET Communications*, 14(15), 2516–2523. doi:10.1049/iet-com.2019.1063
- Mao, Y., Zhang, J., & Letaief, K. B. (2016). Dynamic computation offloading for mobile-edge computing with energy harvesting devices. *IEEE Journal on Selected Areas in Communications*, 34(12), 3590–3605. doi:10.1109/JSAC.2016.2611964
- Min, M., Xiao, L., Chen, Y., Cheng, P., Wu, D., & Zhuang, W. (2019). Learning-based computation offloading for IoT devices with energy harvesting. *IEEE Transactions on Vehicular Technology*, 68(2), 1930–1941. doi:10.1109/TVT.2018.2890685
- Shafique, K., Khawaja, B. A., Sabir, F., Qazi, S., & Mustaqim, M. (2020). Internet of things (IoT) for next-generation smart systems: A review of current challenges, future trends and prospects for emerging 5G-IoT scenarios. *IEEE Access : Practical Innovations, Open Solutions*, 8, 23022–23040. doi:10.1109/ACCESS.2020.2970118
- Shahzadi, R., Niaz, A., Ali, M., Naeem, M., Rodrigues, J. J. P. C., Qamar, F., & Anwar, S. M. (2019). Three tier fog networks: Enabling IoT/5G for latency sensitive applications. *China Communications*, 16(3), 1–11.
- Spinelli, F., & Mancuso, V. (2020). Toward enabled industrial verticals in 5G: A survey on MEC-based approaches to provisioning and flexibility. *IEEE Communications Surveys and Tutorials*, 23(1), 596–630. doi:10.1109/COMST.2020.3037674
- Tang, J., So, D. K. C., Zhao, N., Shojaeifard, A., & Wong, K.-K. (2017). Energy efficiency optimization with SWIPT in MIMO broadcast channels for Internet of Things. *IEEE Internet of Things Journal*, 5(4), 2605–2619. doi:10.1109/JIOT.2017.2785861
- Wang, D., Chen, D., Song, B., Guizani, N., Yu, X., & Du, X. (2018). From IoT to 5G I-IoT: The next generation IoT-based intelligent algorithms and 5G technologies. *IEEE Communications Magazine*, 56(10), 114–120. doi:10.1109/MCOM.2018.1701310
- Wazid, M., Das, A. K., Shetty, S., Gope, P., & Rodrigues, J. J. P. C. (2021). Security in 5G-enabled internet of things communication: Issues, challenges, and future research roadmap. *IEEE Access : Practical Innovations, Open Solutions*, 9, 4466–4489. doi:10.1109/ACCESS.2020.3047895
- Xuefei, E., Ma, Z., & Yu, K. (2020). *Energy-efficient computation offloading and resource allocation in SWIPT-based MEC networks*. IEEE., doi:10.1109/ACCESS.2020.3047690
- Zhang, F., Han, G., Liu, L., Martínez-García, M., & Peng, Y. (2021). Joint optimization of cooperative edge caching and radio resource allocation in 5G-enabled massive IoT networks. *IEEE Internet of Things Journal*, 8(18), 14156–14170. doi:10.1109/JIOT.2021.3068427
- Zhang, J., Du, J., Shen, Y., & Wang, J. (2020). Dynamic computation offloading with energy harvesting devices: A hybrid-decision-based deep reinforcement learning approach. *IEEE Internet of Things Journal*, 7(10), 9303–9317. doi:10.1109/JIOT.2020.3000527
- Zhang, K., Mao, Y., Leng, S., Zhao, Q., Li, L., Peng, X., Pan, L., Maharjan, S., & Zhang, Y. (2016). Energy-efficient offloading for mobile edge computing in 5G heterogeneous networks. *IEEE Access : Practical Innovations, Open Solutions*, 4, 5896–5907. doi:10.1109/ACCESS.2016.2597169

Zhang, Q., Sun, H., Wei, Z., & Feng, Z. (2020, July). Sensing and communication integrated system for autonomous driving vehicles. In *Proceedings of IEEE INFOCOM 2020 —IEEE Conference on Computer Communications Workshops (INFOCOM WKSHPS)*, (pp. 1278–1279). IEEE. doi:10.1109/INFOCOMWKSHPS50562.2020.9162963

Zhou, F., Wu, Y., Hu, R. Q., & Qian, Y. (2018). Computation rate maximization in UAV-enabled wireless-powered mobile-edge computing systems. *IEEE Journal on Selected Areas in Communications*, 36(9), 1927–1941. doi:10.1109/JSAC.2018.2864426